Dynamic Imaging of Nuclear Wave Functions with Ultrashort UV Laser Pulses

André D. Bandrauk[1,2] and Szczepan Chelkowski[1]

[1]*Laboratoire de Chimie Théorique, Faculté des Sciences, Université de Sherbrooke, Sherbrooke, Quebec, Canada J1K 2R1*
[2]*Centre de Recherches Mathématiques, C.P. 6128, Montréal, Quebec, Canada H3C 3J7*

(Received 16 July 2001; published 13 December 2001)

Non-Born-Oppenheimer supercomputer simulations of dissociative ionization of H_2^+ with an ultrashort ($t_p < 15$ fs), intense UV ($\lambda = 30$, 60 nm) laser pulse are used to illustrate the imaging of nuclear motion. The resulting kinetic energy spectra of protons from Coulomb explosion lead by a simple inversion procedure to reconstruction of the initial nuclear probability distribution, i.e., laser Coulomb explosion imaging. Simultaneously, kinetic energy spectra of the ionized electron lead by energy conservation to the same reconstruction of the initial nuclear probability distribution, by laser photoelectron imaging.

DOI: 10.1103/PhysRevLett.87.273004 PACS numbers: 33.80.–b, 32.80.Rm, 42.50.Hz, 42.65.Ky

Modern laser technology and its recent advances are allowing for the generation of light wave packets, i.e., laser pulses, comprising only a few oscillation cycles of the electromagnetic fields, thus giving access to control of high-field interactions with never before achieved precision [1]. If one considers that the time scale of proton motion is between 10–15 fs, such ultrashort pulses will be useful to "clock" the motion of such elusive atoms in molecules. In previous Letters [2,3], we have shown that pulses of duration $t_p < 5$ fs [1], in the near-infrared(IR) region ($\lambda = 800$ nm) and high intensities ($I > 10^{15}$ W/cm^2) could be used to reconstruct the probability distributions of vibrational wave functions of protons in molecules from measured kinetic energy spectra of protons, i.e., by laser Coulomb explosion imaging (LCEI). Such pulses trigger nearly instantaneous complete ionization, followed by approximately classical Coulomb explosion (CE), thus leading to a simple inversion procedure, based on energy conservation during the protons' classical evolution on the repulsive Coulomb potential. We have tested the accuracy of this procedure with the help of non-Born-Oppenheimer simulations [4] of dissociative ionization based on the time-dependent Schrödinger equation (TDSE) describing the electron-proton dynamics of H_2^+ in the laser field. These simulations allow one to compute kinetic energy spectra of exploding protons from the wave function calculated at $t = t_f$, when the protons reach the asymptotic region. Comparison of images reconstructed from these spectra with the initial probability distributions allowed us to conclude that indeed very short pulses, $t_p < 5$ fs, are needed in order to have the faithfully reconstructed stationary probability distributions. Slightly longer pulses, $t_p = 12.8$ fs, led to significant deformation of the reconstructed image, due to laser-induced nuclear motion on Stark-shifted molecular surfaces [3] occurring before the molecule was completely ionized. These Stark shifts are particularly important for intense, near-IR pulses, and they lead to the molecular dissociation via a *bond softening* mechanism [5,6]. In this work we investigate the possibilities for LCEI in the high frequency, ultraviolet (UV) regime, in which one photon transition ionizes directly the molecule and triggers the explosion from the repulsive Coulomb surface, thus avoiding the above distortions occurring in the near-IR regime. As expected, we obtain better quality images of the stationary $v = 2$ state (taken as an example), using considerably longer and less intense pulses than in the long wavelength regime.

Recent experiments [7] and theory [8] show that moving wave packets can be reconstructed as well, with the help of a pump-probe scheme, in which the pump pulse prepares a wave packet and, next, an intense probe laser triggers the Coulomb explosion. Thus, by repeating this experiment for many time delays between the two pulses, we can reconstruct the moving time-dependent wave packet shape from CE ion kinetic energy spectra. We examine here the advantages and limitations of imaging of dissociating wave packets in the UV regime. Our numerical algorithm also allows one to calculate the kinetic energy spectra of ionized electrons [4] from the wave function at $t = t_f$, i.e., when electrons reach the asymptotic region. We find several clear but broad peaks [above threshold ionization (ATI) peaks] in the kinetic energy spectrum of photoelectrons, which have considerably larger widths than ATI peaks in atoms. The phenomenon of ATI has thus far been mostly studied in atoms [9], whereas the experimental data in molecules are rather scarce [5,10] and little theoretical work exists [4]. Several lowest peaks have n-clear nodes corresponding to n nodes of the initial vibrational probability distribution. We show that a simple inversion formula allows also to reconstruct this distribution in a similar way as from the proton kinetic energy spectra. This leads to a new imaging scheme, by laser photoelectron imaging (LPEI), based on the measurement of photoelectron kinetic energy spectra. The scheme works particularly well if one measures the shape of the first peak in electron kinetic spectra, which is the result of a simple one photon absorption process leading to the electron-proton continuum. Consequently, one expects that for sufficiently long laser pulses the photon energy is shared between the electron and the nuclei. Thus, by measuring the shape of the first photoelectron peak, in this high frequency regime, one can reconstruct the shape of the nuclear kinetic energy spectrum and

thus reconstruct the initial nuclear probability distribution, in the same way as by LCEI. Obviously, this scheme of imaging of the wave function, localized in the interval $R_1 < R < R_2$, will work if the photon energy is sufficiently large to allow reaching the continuum via one photon transition from each internuclear distance R in this interval, i.e., we must have $\hbar\omega > e^2/R_1 - E_v$, where $-E_v$ is the ionization energy from the initial vibrational state. We examine here LPEI of dissociating wave packets as well.

Following the procedure described in [4], we have solved, numerically, the complete three-body (1D) TDSE, for the H_2^+ molecule in the field of strong, ultrashort, linearly polarized laser pulses:

$$i\,\frac{\partial\psi(z,R,t)}{\partial t} = H(R,z,t)\psi(z,R,t)\,, \qquad (1)$$

where R is the internuclear distance, z is the electron position (both along the laser polarization vector) with respect to the nuclear of mass, and $H(R,z,t)$ is the three-body Hamiltonian of H_2^+ in the time-dependent laser electric field $E(t)$ [4]. Both electron and nuclei are restricted to move in 1D, along the laser polarization vector, thus allowing one to use very large grids and calculate the kinetic energy spectra of protons and electrons with high precision. We believe that, although reducing the problem to 1D is in general less correct than in the low frequency regime, we still get a reasonably correct spectra for an experiment in which protons and electron are measured in *coincidence,* along the laser polarization vector, since the laser pulses are so short that no molecular rotation occurs during the laser pulse. Simply by measuring protons in this direction, one isolates molecules which remain along the polarization vector during this short interaction time. We assume that at $t = 0$ when the laser pulse is turned on, the H_2^+ molecule is prepared either in the stationary vibrational state $\psi_v(R)\varphi_g(R,z)$ (we have chosen $v = 2$), or in a dissociating state (with momentum p_0) on the ungerade electronic surface $^2\Sigma_u^+$, i.e., $\psi(R,z,0) = \psi_G(R)\varphi_u(R,z)$, where $\varphi_g(R,z)$ and $\varphi_u(R,z)$ are the electronic gerade and ungerade eigenfunctions, respectively, and $\psi_G(R)$ is simply a normalized Gaussian function, multiplied by a factor $\exp(ip_0R)$. The Gaussian function was centered at $R = R_0$ and its square had a half-width $R_H = 4.2$ bohrs. The wave packet momentum was set to $p_0 = \sqrt{2\mu E_p}$, where E_p is the energy of a dissociating Gaussian wave packet (we used $E_p = 0.37$ eV). We used the laser electric field $E(t) = E_0(t)\sin(\omega t)$, with a Gaussian-like envelope (i.e., a Gaussian having the experimental intensity profile with a half-width t_p, but having a finite total duration $t_{\rm tot} = 4t_p$ and the peak at $t_{\rm tot}/2$). We have performed a series of simulations with the laser intensity $I = 10^{15}\mathrm{W/cm^2}$ and for two different wavelengths $\lambda = 32$ (for the $v = 2$ vibrational wave function imaging case) and $\lambda = 60$ nm for the case of imaging a dissociating wave packet. In each case, the time evolution of the wave function $\psi(z,R,t)$ was carried on until the wave packet of exploding protons has reached the distance $R > 40$ a.u. Then the kinetic energy spectrum of exploding protons $S_N(E_N)$ (where E_N is the total nuclear kinetic energy in the protons c.m. system) was calculated by projecting the resulting final wave function $\psi(R,z,t_{\rm final})$ onto the exact Coulomb waves [2,8] $\varphi_C(E_N,R)$ and next integrating out the electron z coordinate. The wave function splitting technique used in our time-evolution algorithm [4] allows us to calculate the electron kinetic energy spectrum $S_e(E_e)$ (ATI spectrum) from the exact wave function at final time t_f (after integrating out the proton R variable [2]). We plot in Fig. 1a the proton kinetic energy spectra $S_N(E_N)$ and in Fig. 1b electron ATI spectra $S_e(E_e)$ for relatively long laser pulses, $t_p = 12.8$ fs (as compared to $t_p = 3.2$ fs used in our previous work in the $\lambda = 800$ nm regime [4]). Both spectra show clearly two nodes and three peaks which are clear imprints of the initial spatial probability distributions of the $v = 2$ vibrational state. In general, there is no simple mapping between $S_N(E_N)$ and the initial nuclear function at $\psi_v(R)$; in our previus work (in the near-IR regime), we used the inversion procedure based on the assumption that complete ionization was nearly instantaneous and $|\psi_v(R)|^2$ was reconstructed via energy conservation during proton classical evolution on the repulsive Coulomb potential. In the UV regime, the imaging procedure does not require complete ionization and we derive it using the Fermi golden rule (FGR) for the one photon

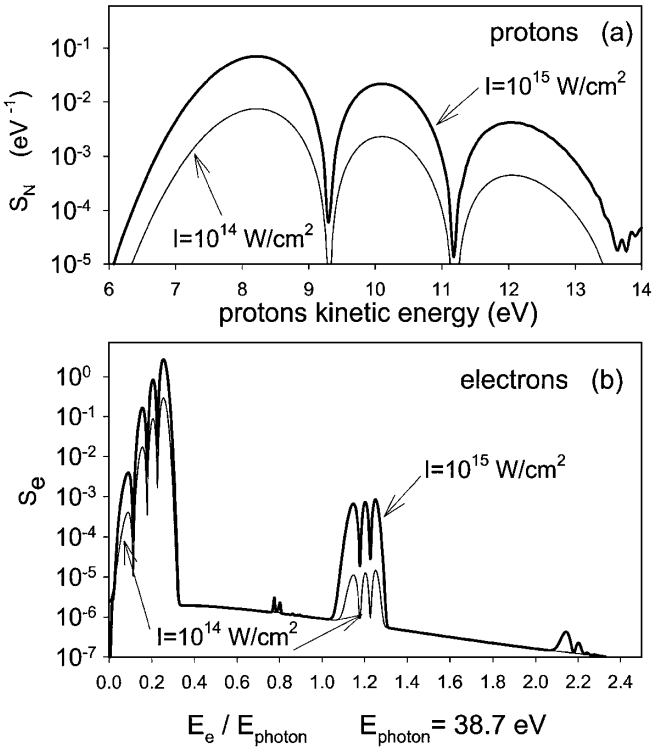

FIG. 1. (a) Total Coulomb explosion kinetic energy spectrum of protons; (b) photoelectron, ATI, kinetic energy spectra. Both are for wavelength $\lambda = 32$ nm, laser intensity $I = 10^{15}$ W/cm^2, and pulse duration $t_p = 12.8$ fs. H_2^+ was prepared in the ground vibrational $v = 2$ state at the beginning of the simulation. We also show spectra for lower intensity, $I = 10^{14}$ W/cm^2, $t_p = 25.6$ fs (thin line).

transition to electron-proton continua and the reflexion approximation [3], which lead to following mappings of experimental nuclear spectra [11]:

$$|\psi_{\mathrm{LCEI}}(R_I)|^2 = S_N(E_N)\,\frac{q^2}{R_I^2 T(R_I,E_e)t_p}\,, \qquad (2)$$

where $E_e = \hbar\omega + E_v - E_N$. Alternatively, when the electron kinetic energy spectrum $S_e(E_e)$ is measured, after integration over nuclear E_N in FGR, we get

$$|\psi_{\mathrm{LPEI}}(R_I)|^2 = S_e(E_e)\,\frac{q^2}{R_I^2 T(R_I,E_e)t_p}\,, \qquad (3)$$

where $E_N = \hbar\omega + E_v - E_e$, $R_I = q^2/E_N$. In both cases, we used $R_I = q^2/E_N$ and $E_{v=2} = -20.6$ eV. Note that, in both above equations, we should divide the spectrum by the ionization rates $T(R_I, E_e)$ for H_2^+ in which the nuclei have a fixed internuclear distance. These rates may strongly vary as a function of R_I (see inset of Fig. 2a) and may cause difficulties when imaging in the perturbative UV regime [11]. Since experimentalists in general will not have the access to this R-dependent rate, we simplify the imaging procedure and simply replace the factor $T(R_I, E_e)t_p$ in the above formulas by the R-independent probability of ionization P_I which is the area under spectra shown in Fig. 1. We display in Fig. 2a the resulting initial nuclear probability distribution shape $|\psi_{\mathrm{LCEI}}(R_I)|^2$ reconstructed from the nuclear kinetic energy spectrum

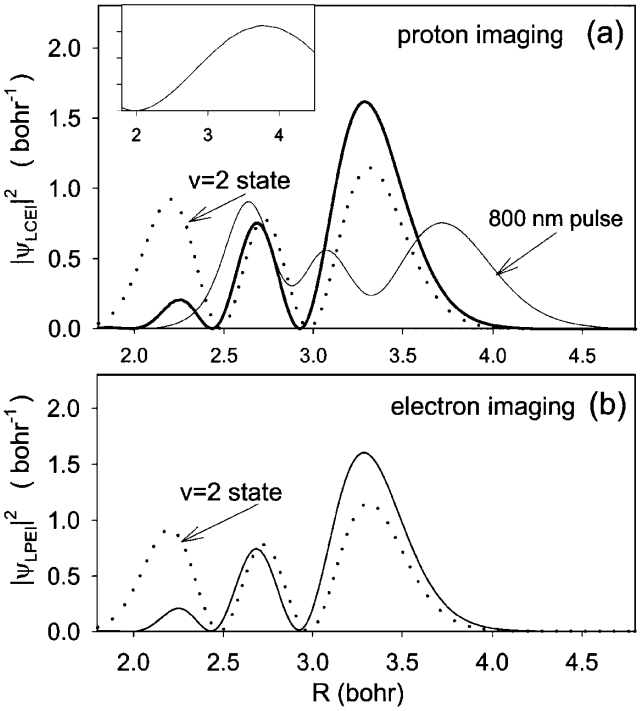

FIG. 2. UV imaging from spectra in Fig. 1: (a) LCEI $|\psi_{\mathrm{LCEI}}|^2$, (b) LPEI $|\psi_{\mathrm{LPEI}})|^2$, of $|\psi_{v=2}(R)|^2$ (dotted line). The image $|\psi_{\mathrm{LCEI}}|^2$ obtained using the 800 nm, $t_p = 12.8$ fs, $I = 4 \times 10^{15}$ W/cm^2 laser pulse is also shown in (a) as a thin line. The inset in (a) shows the ionization rate $T(R)$ (arbitrary units, linear scale) as a function of R in bohrs.

$S_N(E_N)$ (shown in Fig. 1a) with the help of Eq. (2), whereas in Fig. 2b we show $|\psi_{\mathrm{LPEI}}(R_I)|^2$ reconstructed from the electron kinetic energy spectrum $S_e(E_e)$, using (3). We note that the first peak is too low, which is caused by the R-dependent ionization rate, displayed in the inset of Fig. 2a. Note, however, that the node locations are very exactly reproduced. We observe that this imaging procedure is much more precise in the high frequency regime than in the long wavelength regime, $\lambda = 800$ nm, studied previously [3]. We display in Fig. 2a the initial probability distribution reconstructed from the spectrum obtained at 800 nm (thin line) for the same duration of the laser pulse, i.e., $t_p = 12.8$ fs. The precision of imaging with the high frequency laser is much better than even for the case of a very short pulse, $t_p = 3.2$ fs, 800 nm, discussed in [2]. Clearly, the laser induced bond softening dynamics leads to considerable distortions in the imaging process at low frequencies and therefore requires shorter pulses ($t_p < 5$ fs). Practically no deformation occurs for $t_p = 12.8$ fs pulses in the high frequency regime, since the one photon absorption mechanism leads the electron directly to the continuum, without initiating any dynamics within H_2^+ during the ionization process. We used very high intensities, $I = 10^{15}$ W/cm^2, for imaging shown in Fig. 2 in order to show that higher order peaks show also imprints of the $v = 2$ state nodes. Since such high intensity UV laser pulses are not currently achievable in UV, we show in Fig. 1 (thin lines) spectra obtained using the lower intensity, $I = 10^{14}$ W/cm^2, laser pulses. Both proton and electron kinetic energy spectra remain identical in structure, thus confirming the feasibility of LCEI and LPEI at lower intensities as well. We have also calculated Coulomb explosions and ATI spectra resulting from dissociating wave packets, which can be prepared, for instance, with the help of a relatively low intensity (pump) laser pulse (e.g., $I < 5 \times 10^{13}$ W/cm^2, such that ionization of H_2^+ is negligible) preceding the UV laser (probe) pulse triggering the Coulomb explosion [7,8]. Our initial wave packet was a Gaussian localized at $R = R_0$, and moved with the kinetic energy $E_p = 0.37$ eV. We illustrate in Fig. 3 the imaging of moving wave packets, using very short, $t_p = 3.2$ fs, $\lambda = 60$ nm lase pulses. This wavelength is short enough for imaging via one photon ionization at $R > 10$ bohrs. First, we have calculated the proton and electron energy spectra and, next, we computed the images $|\psi_{\mathrm{LCEI}}(R_I)|^2$ and $|\psi_{\mathrm{LPEI}}(R_I)|^2$ using the inversion procedures (2) and (3), with E_v replaced by $-I_H$, where $I_H = 18.2$ eV (which is the ionization potential of a 1D hydrogen atom), and E_N is replaced by $E_N - E_p$. We also plot, for comparison, in Fig. 3a (thin line), $|\psi_{\mathrm{LCEI}}(R)|^2$ obtained from proton spectra calculated using 800 nm ($t_p = 3.2$ fs, $I = 4 \times 10^{14}$ W/cm^2) laser pulses. We note that in the near-IR regime the reconstructed image is broader due to energy transfer from laser to nuclei, resulting from much higher ponderomotive energy of electron and proton [8]. Clearly, both schemes, LCEI and LPEI, allow to measure the wave packet motion in the UV regime, although LPEI peaks overlap and are too large, for $t_p = 3.2$ fs. This

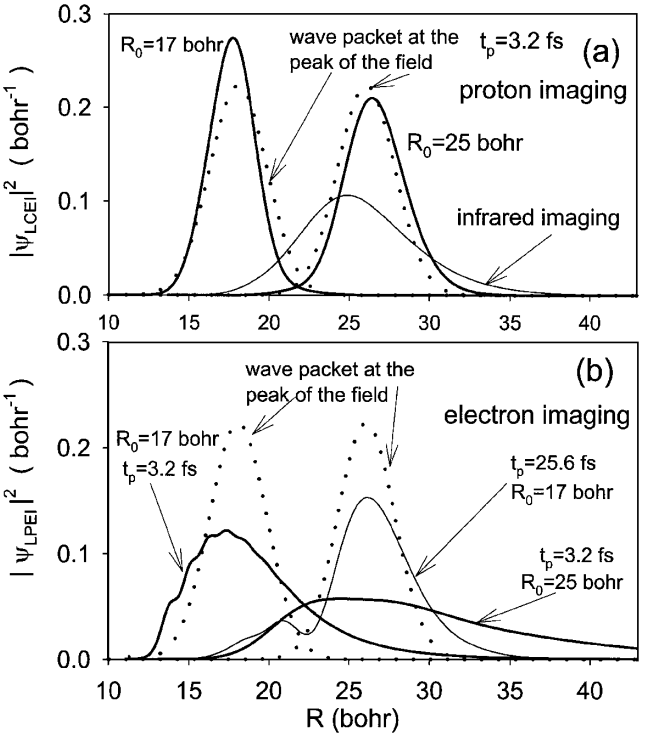

FIG. 3. (a) LCEI: $|\psi_{\mathrm{LCEI}}(R_I)|^2$; and (b) LPEI: $|\psi_{\mathrm{LPEI}})|^2$; of a dissociating Gaussian wave packet $|\psi_G(R)|^2$. Results of three simulations are shown, the first with $R_0 = 17$ bohrs and the second with $R_0 = 25$ bohrs, both with $t_p = 3.2$ fs pulse (thick lines). The third was done with a $t_p = 25.6$ fs pulse, initialized with $R_0 = 17$ bohrs [thin line in (b)]. The wave-packet shapes at the pulse maximum are also displayed (dotted lines). In all cases: $\lambda = 60$ nm. $I = 10^{15}$ W/cm^2, $E_p = 0.37$ eV. We show in (a) results of imaging for 800 nm laser pulses, $t_p = 3.2$ fs, $I = 4 \times 10^{15}$ W/cm^2 (thin line).

is related to a large spectral width of the laser pulse, $\Delta\omega = 0.6$ eV, which is even larger than the energy separation of peaks in Fig. 3a, equal to 0.5 eV, thus leading to corrections to Eq. (3) beyond the Fermi golden rule. Since our wave packet moves with the speed $v_p = 0.22$ bohrs/fs, we expect that longer pulses, e.g., $t_p = 25.6$ fs still will allow one to resolve the wave packet movement and to reduce the above-mentioned problems with LPEI for too short pulses. We have calculated the electron spectra using the $t_p = 25.6$ fs laser pulse, initialized with a Gaussian centered at $R_0 = 17$ bohrs and repeated the same inversion procedure, as in Fig. 3b. The resulting image $|\psi_{\mathrm{LCEI}}|^2$ is shown in Fig. 3b (thin line). Clearly, the reconstructed shape using LPEI with a longer pulse is closer to the exact shape of the wave packet (dotted line) than in the case of a shorter pulse. Note however, that because the wave packet displacement during the pulse rise the image (thin line) is considerably displaced from the initial position $R_0 = 17$ bohrs, due to 8 times longer rise time of the pulse. The longer pulses will not lead to better LPEI imaging since already with the $t_p = 25.6$ fs pulse the wave packet motion leads to a blur of the order $t_p v_p = 5.6$ bohrs. This blur manifests itself as a long tail seen at small R (thin line) in Fig. 3b. We illustrate the effects of pulse length and effects due to R-dependent rates $T(R)$ (e.g., a dip in Fig. 3b, thin line) on the quality of the image in more detail in a longer paper [11].

In summary, we have demonstrated that UV ultrashort, intense laser pulses allow one to monitor the nuclear motion, with similar or better accuracy and with longer pulses than in the case of the previously discussed near-IR regime [2,3], since the dominant ionization mechanism in the UV regime is direct one photon ionization which does not lead to any distortion related to Stark shifts of molecular surfaces. UV ultrashort pulses lead to excellent LCEI imaging of *dynamic* (e.g., dissociative) proton motion, whereas LPEI is less accurate due to large energy bandwidth of such pulses (Fig. 3b). Pulses of duration $t_p = 10-15$ fs (depending on the speed of the moving structure) seem to be optimal as they give comparably accurate dynamic LCEI and LPEI proton distributions. Imaging of stationary structures using UV pulses can be done with much longer and less intense laser pulses, as expected from the Fermi golden rule, in contrast with the low frequency regime where intense and shorter pulses are required; however, some image distortions may occur in the UV low intensity regime due to the R dependence of ionization rates $T(R)$. There is no minimum theoretical UV laser intensity for LCEI and LPEI, if LPEI is based on the lowest photoelectron peak, since both are based on the Fermi golden rule for the one photon process, which falls linearly as a function of intensity. Clearly, Fig. 1 shows this linear, perturbative behavior.

We thank the Natural Sciences and Engineering Research Council of Canada (NSERC) and the Canadian Institute for Photonics Innovation (CIPI) for the financial support. We also thank Maui High Performance Computing Center for computer time on IBM-SP2.

[1] T. Brabec and F. Krausz, Rev. Mod. Phys. **72**, 545 (2000).
[2] S. Chelkowski, P. B. Corkum, and A. D. Bandrauk, Phys. Rev. Lett. **82**, 3416 (1999).
[3] A. D. Bandrauk and S. Chelkowski, Chem. Phys. Lett. **336**, 518 (2001).
[4] S. Chelkowski, C. Foisy, and A. D. Bandrauk, Phys. Rev. A **57**, 1176 (1998).
[5] P. H. Bucksbaum *et al.,* Phys. Rev. Lett. **64**, 1883 (1990).
[6] A. D. Bandrauk *et al.,* in *Molecules in Laser Fields,* edited by A. D. Bandrauk (Dekker, New York, 1994), Chap. 3.
[7] H. Stapelfeldt, E. Constant, and P. B. Corkum, Phys. Rev. Lett. **74**, 3780 (1995).
[8] S. Chelkowski and A. D. Bandrauk (to be published).
[9] M. Gavrila, *Atoms in Intense Laser Fields* (Academic, New York, 1992).
[10] J. W. J. Verschuur *et al.,* Phys. Rev. A **40**, 4383 (1989); C. Cornaggia *et al.,* Phys. Rev. A **34**, 207 (1986).
[11] S. Chelkowski and A. D. Bandrauk (to be published).